Planta (1998) 205: 39–50

Planta

Distribution and dynamics of the cytoskeleton in graviresponding protonemata and rhizoids of characean algae: exclusion of microtubules and a convergence of actin filaments in the apex suggest an actin-mediated gravitropism

Markus Braun[1,2], Geoffrey O. Wasteneys[2]

[1]Botanisches Institut, Universität Bonn, Venusbergweg 22, D-53115 Bonn, Germany
[2]Plant Cell Biology Group, Research School of Biological Sciences, The Australian National University, GPO Box 475, 2602 Canberra ACT, Australia

Received: 14 September 1997 / Accepted: 16 October 1997

Abstract. The organization of the microtubule (MT) and actin microfilament (MF) cytoskeleton of tip-growing rhizoids and protonemata of characean green algae was examined by confocal laser scanning microscopy. This analysis included microinjection of fluorescent tubulin and phallotoxins into living cells, as well as immunofluorescence labeling of fixed material and fluorescent phallotoxin labeling of unfixed material. Although the morphologically very similar positively gravitropic (downward growing) rhizoids and negatively gravitropic (upward growing) protonemata show opposite gravitropic responses, no differences were detected in the extensive three-dimensional distribution of actin MFs and MTs in both cell types. Tubulin microinjection revealed that in contrast to internodal cells, fluorescent tubulin incorporated very slowly into the MT arrays of rhizoids, suggesting that MT dynamics are very different in tip-growing and diffusely expanding cells. Microtubules assembled from multiple sites at the plasma membrane in the basal zone, and a dense subapical array emerged from a diffuse nucleation centre on the basal side of the nuclear envelope. Immunofluorescence confirmed these distribution patterns but revealed more extensive MT arrays. In the basal zone, short branching clusters of MTs form two cortical hemicylinders. Subapical, axially oriented MTs are distributed in equal density throughout the peripheral and inner cytoplasm and are closely associated with subapical organelles. Microtubules, however, are completely absent from the apical zones of rhizoids and protonemata. Actin MFs were found in all zones of rhizoids and protonemata including the apex. Two files of axially oriented bundles of subcortical actin MFs and ring-like actin structures in the streaming endoplasm of rhizoids were detected in the basal zones by microinjection or rhodamine-phalloidin labeling. The subapical zone contains a dense array of mainly axially oriented actin MFs that co-distribute with the subapical MT array. In the apex, actin MFs form thicker bundles that converge into a remarkably distinct actin patch in the apical dome, whose position coincides with the position of the endoplasmic reticulum aggregate in the centre of the Spitzenkörper. Actin MFs radiate from the actin patch towards the apical membrane. Together with results from previous inhibitor studies (Braun and Sievers, 1994, Eur J Cell Biol 63: 289–298), these results suggest that MTs have a stabilizing function in maintaining the polar cytoplasmic and cytoskeletal organization. The motile processes, however, are mediated by actin. In particular, the actin cytoskeleton appears to be involved in the structural and functional organization of the Spitzenkörper and thus is responsible for controlling cell shape and growth direction. Despite the similar structural arrangements of the actin cytoskeleton, major differences in the function of actin MFs have been observed in rhizoids and protonemata. Since actin MFs are more directly involved in the gravitropic response of protonemata than of rhizoids, the opposite gravitropism in the two cell types seems to be based mainly on different properties and activities of the actin cytoskeleton.

Key words: Actin microfilament – Characean algae (rhizoids, protonemata) – Gravitropism – Microtubule – Microinjection – Tip growth

Introduction

Rhizoids and protonemata of characean algae are tube-like, tip-growing cells, highly specialized to penetrate mud and soil. Rhizoids grow positively gravitropically (downward) to anchor the green thallus in the sediment. Protonemata, which develop in darkness, grow negatively gravitropically (upward) in order to regenerate the complex organized, multicellular green plant

Abbreviations: FITC = fluorescein isothiocyanate; MF = microfilament; MBS = *m*-maleimidobenzoic acid N-hydroxysuccinimide ester; MT = microtubule

Correspondence to: M. Braun;
E-mail: unb13A@ibm.rhrz.uni-bonn.de; Fax: 49 (228) 73 2677

(Pickett-Heaps 1975; Hodick 1993). Both cell types, which arise either from meristem-like nodal cells or from zygotes, are polarly organized and very similar in general shape and cytoplasmic zonation (Hodick 1993). Their opposite gravitropic responses are both dependent on sedimentable statoliths, whose position and transport is dynamically controlled by the actin cytoskeleton (Sievers et al. 1991b; Buchen et al.1993; Braun and Sievers 1993; Hodick 1994). The presence of actin in rhizoids has been demonstrated by rhodamine phalloidin labeling (Sievers et al.1991a; Braun and Sievers 1993). Inhibitor-induced disassembly of the actin microfilament (MF) system (Braun and Sievers 1993) resulted in the sedimentation of the statoliths onto the apical cell wall and caused cessation of tip growth (Hejnowicz and Sievers 1981) and disintegration of the tip-growth-organizing complex, the Spitzenkörper (Bartnik and Sievers 1988). These observations suggest that actin is involved in the mechanism of strictly tip-focused exocytosis of secretory vesicles and also structurally organizes and stabilizes the Spitzenkörper in the apical dome of rhizoids and protonemata. At the ultrastructural level, the Spitzenkörper in rhizoids and protonemata is characterized by a unique aggregation of endoplasmic reticulum (ER) membranes, a great number of secretory vesicles and microvesicles (Bartnik and Sievers 1988; D. Hodick, Botanisches Institut, Universität Bonn, personal communication). The ER aggregation is located very close to the outermost apical membrane, the centre of maximal growth, and appears to be involved in the actomyosin-mediated guiding of the secretory vesicles (Bartnik et al. 1990) and, therefore, in the control of gravity-oriented tip growth.

In order to shed light on the involvement of cytoskeletal elements in the gravitropic component of tip growth, we examined the structural three-dimensional organization of actin MFs and microtubules (MTs) in further detail. Because of the absence of MTs in the apical zone, it is most likely that they do not play a direct role in graviperception and graviresponse (Braun and Sievers 1994). Differences in transport and sedimentation behaviour of the statoliths in protonemata and rhizoids and the different features of the growth responses suggest that actin might play a specific but different role in the opposite gravitropic response of the two cell types (Hodick 1994; Braun 1996a).

Conventional epifluorescence microscopy has identified certain features of the actin (Sievers et al. 1991a) and MT (Braun and Sievers 1994; Braun 1997) arrays in characean rhizoids. Specifically, the application of rhodamine phalloidin to unfixed material or chemical fixation followed by anti-actin immunofluorescence revealed arrays of actin bundles in the subcortical basal cytoplasm and a dense actin network throughout the apical and subapical cytoplasm (Sievers et al. 1991a). Immunofluorescence has also been used to label microtubules in the cortical basal cytoplasm as well as a dense, axially oriented MT network in the subapical zone (Braun and Sievers 1994; Braun 1997). However, conventional fluorescence microscopy failed to reveal any features of the cytoskeleton in the inner cytoplasm of the apical and subapical zones because of high background fluorescence. In the present paper, the three-dimensional organization of actin MFs and MTs in rhizoids has been re-examined by confocal laser scanning microscopy after microinjection of fluorescent tubulin and phallotoxins or labeling with rhodamine phalloidin and cytoskeleton-specific antibodies. The distribution of the actin and MT cytoskeleton in protonemata was also documented for the first time. Improved visualization methods and optical sectioning reveal the most complex cytoskeletal organization presented in any tip-growing cell so far and microinjection gives the first insights into the dynamic behaviour of the cytoskeleton in live, gravitropically tip-growing cells.

Material and methods

Culture of rhizoids. *Chara globularis* (Thuill.) and *Nitella pseudoflabellata* (A. Br. & Nordst. em. R.D.W.) were collected from the Shoalhaven River catchment between Bungonia and Bungendore, in the southern tablelands of New South Wales, Australia and cultured in 5- or 10-l beakers as described by Wasteneys and Williamson (1989). Young rapidly growing shoots were cut into short segments of at least two nodes and one internodal cell. For the production of protonemata, the segments were embedded in a thin layer of agar (1.2% in distilled water) on a microscope slide, covered with long coverslip and fixed at two sides with tape. These cuvettes were placed horizontally in staining jars filled with modified Forsberg medium (Wasteneys et al. 1996). Protonemata developed within 15–20 d in complete darkness at room temperature (21–23 °C). To induce formation of rhizoids, shoot segments were placed in upright flat culture chambers (330 ml) containing modified Forsberg medium at room temperature under continuous incandescent white light.

Immunofluorescence labeling. Small pieces of agar containing nodes with dark-grown protonemata were cut and placed for 20 min in a fixative solution of 1% formaldehyde and 1% glutaraldehyde (Sigma, St. Louis, Mo, USA; Grade I, stored at −20 °C) in microtubule-stabilizing buffer (MSB) containing 50 mM Pipes, 5 mM EGTA and 5 mM $MgSO_4$ (pH 7.2). Bundles of rhizoids were fixed by first removing them from the culture chambers and directly transferring them to the fixative solution. Some rhizoids were placed horizontally for 12 and 20 min prior to fixation. Alternatively, specimens were pretreated with MBS (*m*-maleimidobenzoyl-N-hydroxysuccinimide ester; Boehringer, Mannheim, Germany; 20–200 μM in Forsberg medium) for 5 min and 10 min. After several rinses in MSB, the buffer was gradually replaced with phosphate-buffered saline (PBS). Following washing in PBS the cells were treated three times with freshly prepared 1 mg · ml^{-1} $NaBH_4$ for 10 min, washed again in PBS and transferred to permeabilization buffer (1% Triton X-100 in PBS, pH 7.4) for 30 min. Protonemata were removed from the agar, placed on microscope slides and frozen immediately in liquid nitrogen for 1 or 2 min. Frozen cells were carefully squashed between a pre-chilled coverslip and the microscopic slide (freeze cracking or shattering, see Braun and Sievers 1994). After thawing and washing three times in PBS containing 50 mM glycine, the cells were incubated with the antibodies for 2 h to overnight at 37 °C. After three rinses in the same buffer, the cells were incubated with fluorescein isothiocyanate (FITC)-conjugated second antibodies for 2 h at 37 °C. Stained cells were rinsed three times with PBS and mounted in 0.1% *p*-phenylene diamine and 50% glycerol to minimize fading of the fluorescent conjugate.

Microtubules were labeled with monoclonal mouse anti-tyrosine α-tubulin, clone TUB-1A2 (Sigma T-9028; 1:800). For actin labeling, the C4 monoclonal antibody raised against chicken

gizzard actin (Lessard 1988) was used at a dilution of 1:100. The FITC-conjugated anti-mouse IgG (Silenus, Hawthorn, Victoria, Australia; 1:100) served as a secondary antibody for both monoclonal antibodies.

For double labeling of microtubules and actin, cells were sequentially incubated in clone TUB-1A2 (Sigma; 1:800), biotinylated goat anti-mouse IgG (Sigma; 1:100), mouse anti-actin IgM clone N350 (Amersham, Sydney, Australia; 1:100), secondary antibody (Sigma F-9259; 1:40) specific to mouse IgM and finally in Avidin Neutralite Texas Red (Molecular Probes, Eugene, Ore., USA; 1:100). In order to enhance the avidin fluorescence, 10 μM biotin, diluted in PBS, was added as a last incubation step. Cells were washed three times with incubation buffer between each incubation step. For double-labeling of microtubules and DNA, cells were labeled for 1 h each with TUB 1A2 (Sigma), FITC-conjugated anti-mouse IgG (Silenus) and finally incubated for 15 min in 2 $\mu g \cdot ml^{-1}$ propidium iodide (Sigma; P-4170), diluted in PBS. For double labeling of actin and DNA, clone C4 anti-actin (ICN), anti-mouse IgG FITC-conjugate (Silenus) and propidium iodide were used.

Microinjection and confocal laser scanning microscopy. The probes FITC-phalloidin and Bodipy FL phallacidin (Molecular Probes) were diluted in methanol to a concentration of 6.6 μM and kept frozen until use. Prior to microinjection, methanol was removed from aliquots of 20 μl by desiccation. The injection dilution of 0.66 μM was prepared by adding 100 mM KCl, sonicated and centrifuged (5 min at 10 000 *g*).

Tubulin extraction and labeling with 5(6)-carboxyfluorescein-N-hydroxysuccinimide ester (Boehringer) was performed as described by Wasteneys et al. (1993) according to the method of Vigers et al. (1988) with the modifications of Zhang et al. (1990). Freshly thawed tubulin, which was frozen as a stock solution at −80 °C at a concentration of 10 $mg \cdot ml^{-1}$ in buffer containing 20 mM sodium glutamate, 0.5 mM $MgSO_4$ and 1 mM EGTA, was diluted to 5 $mg \cdot ml^{-1}$ in injection buffer containing 1 mM GTP. Microinjection was performed on rhizoids, which were immobilized with low-gelling agarose, using hydraulic-pressure micropipettes (Hepler et al. 1993) mounted on a Zeiss Axiovert IM-10 coupled to a confocal laser scanning system (MRC-BioRad 600; Microscience Division, Hemel Hempstead, UK). Images of fluorescently labeled cells were collected using Kalman filtering of 6–10 scans. Digital images were processed with Confocal Assistant software (CAS, version 3.10) and printed on Epson Stylus Color 800 and Tectronix Phaser 440.

Rhodamine phalloidin labeling. Small aliquots (20 μl) of 6.6 μM rhodamine phalloidin (Molecular Probes) prepared in methanol were diluted in 0.2 M sodium potassium phosphate buffer (pH 7.2) to a 30 nM working solution. For labeling, rhizoids and protonemata were incubated in a drop of rhodamine phalloidin solution on a microscope slide without pre-fixation and examined with the confocal laser scanning microscope.

Results

Actin cytoskeleton in rhizoids

The three-dimensional organization of the actin cytoskeleton of rhizoids was examined using rhodamine phalloidin staining, indirect immunofluorescence and microinjection of live cells with fluorescently labeled phalloidin and phallacidin. Confocal laser scanning microscopy allowed optical sectioning which was indispensable for resolving the fine fibrous structures of the actin MFs in the apical and subapical zones of rhizoids.

Rhodamine phalloidin labeling revealed an extensive array of actin MFs in predominant axial orientation in the subapical and apical zone (Fig. 1). The subapical zone was characterized by an extremely dense and homogeneous network of actin MFs of equal density in the peripheral and inner cytoplasm (Figs. 1, 2). The very thin (0.4 μm) optical section image (Fig. 2) illustrates the dense subapical actin MF network encircling the organelles. In the apical zone (Fig. 1, zone between the two arrowheads), MFs form less densely packed but relatively thick bundles that run between the numerous statoliths (Fig. 1A,S) and converge into a brightly fluorescing patch-like actin array (Fig. 1B, arrow) localized at a close, constant distance from the outermost tip, the area of maximal growth. The fine fibrous appearance of the actin patch, which has a diameter of 5–8 μm, is shown in two sequential median optical sections (Fig. 1B,C). Actin MFs radiate from the actin patch towards the plasma membrane of the apical dome. They are not, however, linked head-on to the plasma membrane. Most of these apically radiating actin MFs curve fountain-like before reaching the apical membrane, merge into thicker bundles and return towards the base of the cell along the cell periphery. Actin labeling in plasmolysed rhizoids (Fig. 3) demonstrates that the actin MFs emerging from the actin patch are linked only very weakly or dynamically to the apical plasma membrane. After labeling with rhodamine phalloidin solution containing 0.2–0.4 M sorbitol, the apical plasma membrane became detached from the apical cell wall (Fig. 3A, arrowhead). The actin cytoskeleton including the actin patch (Fig. 3B, arrow) together with the statoliths, however, retracted as a complex even further than the apical plasma membrane (Fig. 3B, arrowhead).

In rhizoids, anti-actin immunofluorescence with and without MBS pretreatment revealed the same overall pattern of the actin cytoskeleton as phallotoxin labeling, namely, the distinct differences between the subapical and apical actin arrays and the conspicuous patch-like actin array in the centre of the apical dome (Fig. 4A). Concentrations of MBS low enough not to cause any disruption of MTs (cf. Collings et al. 1995) and subsequent breakdown of the cytoplasmic zonation only slightly improved the preservation of actin. Nevertheless, after chemical fixation and immunofluorescence labeling, the actin arrays were less extensive than after rhodamine phalloidin staining. In particular, the apical MF bundles were less numerous and less net-like in chemically fixed and immunofluorescently labeled rhizoids.

To study the effect of reorientation on the distribution of actin MFs, rhizoids were placed horizontally for 12 min and 20 min prior to fixation and antibody labeling. After 12 min, the statoliths had already completely sedimented onto the lower cell flank, but gravitropic bending had not yet started. Horizontal exposure for 20 min was sufficient to induce a slight downward gravitropic curvature. No differences could be observed in the symmetric arrangement of the immunofluorescently labeled actin MFs in rhizoids that remained vertically positioned (Fig. 4A) and in rhizoids growing horizontally for 12 min and 20 min (Fig. 4B,C). Clearly, the sedimenting statoliths can

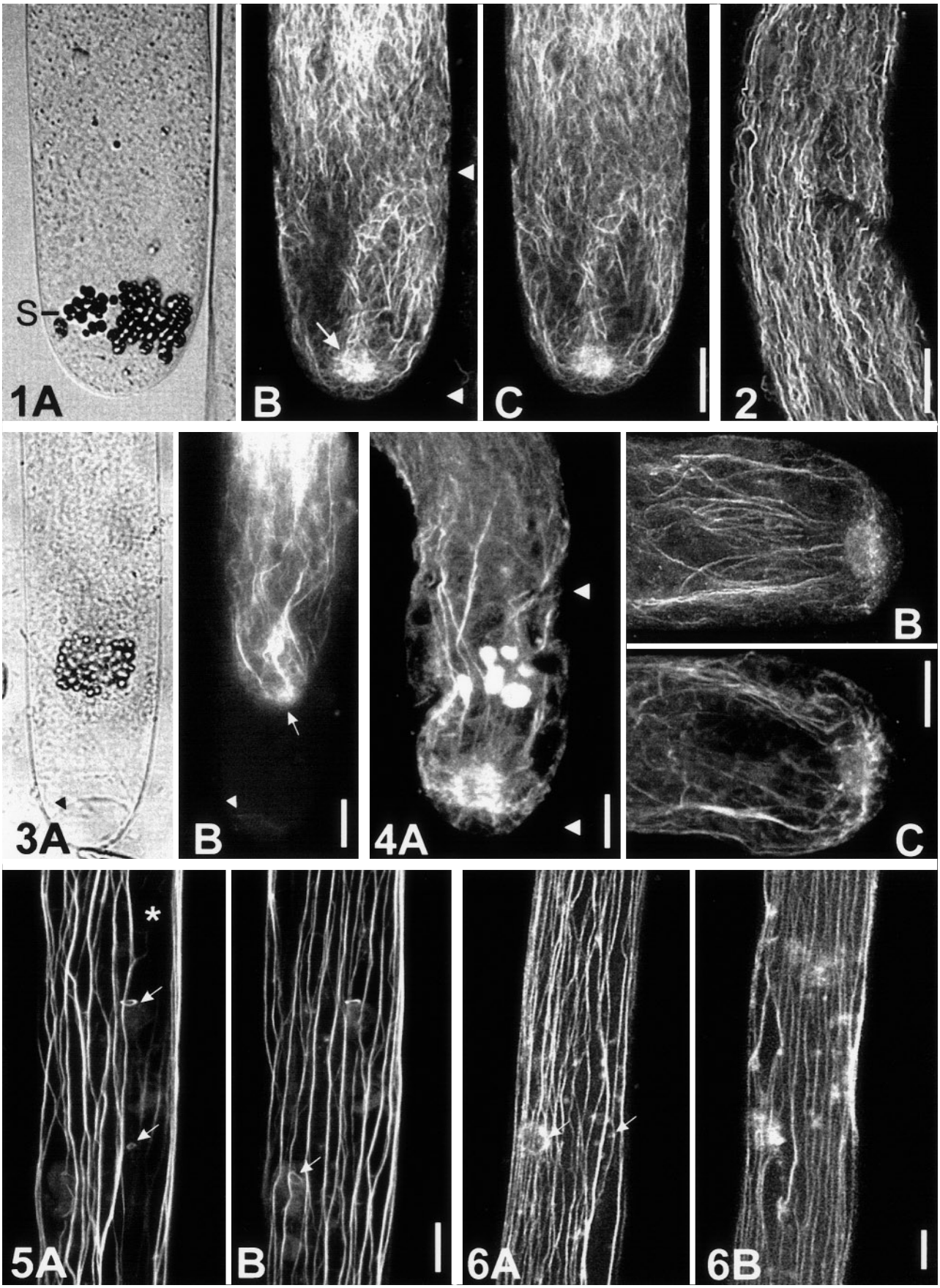
S
1A
B
C
2
3A
B
4A
B
C
5A
B
6A
6B

Figs. 1–6. Distribution of actin MFs in *Chara* rhizoids. All scale bars = 10 μm

Fig. 1A–C. Micrographs of the apical zone (region between the *arrowheads*) and part of the subapical zone of a rhodamine phalloidin-labeled rhizoid. **A** The differential interference contrast (DIC) image corresponding to the fluorescence images shows numerous statoliths (*S*) in their usual location. **B, C** Two sequential mid-plane optical sections (0.8 μm interval) showing the actin MF organization in the apical and part of the subapical zone. Note the loose arrangement of the apical actin MFs that converge into an apical brightly fluorescing patch-like actin array (*arrow*). Actin MFs radiating towards the apical plasma membrane curve before reaching the apical membrane and merge into thicker MF bundles running basipetally. Optical section thickness = 0.6 μm

Fig. 2. Actin MF organization in the subapical zone of a rhodamine phalloidin-labeled rhizoid. Cytoplasmic organelles (dark spheres) are embedded in extremely numerous axially oriented actin MFs. Projection of four serial images at 0.4-μm intervals

Fig. 3A,B. Rhizoid after labeling with rhodamine phalloidin solution containing 0.4 M sorbitol. **A** The DIC image showing the detachment of the apical plasma membrane (*arrowhead*) from the cell wall of the apical dome. **B** The corresponding conventional fluorescence image shows that the actin cytoskeleton, including the apical actin patch (*arrow*), is completely disconnected from the apical membrane (*arrowhead*) and together with the actin-embedded statoliths is retracted from the apical dome

Fig. 4A–C. Anti-actin immunofluorescence reveals a dense network of actin MFs in the subapical zone and more strongly fluorescent, less-reticulate actin MF bundles in the apical zone (region between the *arrowheads*) radiating from apical actin patches. **A** Actin MF distribution in a downward-growing rhizoid containing statoliths (*white spheres*) in their original position. After 12 min (**B**) and 20 min (**C**) in a horizontal position, no major redistribution of actin MFs is visualized in the apical zones; they are still symmetrically arranged and the actin patches are not displaced from their central position in the graviresponding tip. Optical section images of 1 μm thickness

Fig. 5A,B. Actin bundles in the basal zone of rhizoids labeled with rhodamine phalloidin. Projections of 12 serial images at 0.8-μm intervals showing the actin bundles in the first (**A**) and second (**B**) half of the basal cell cylinder. Note the actin rings associated with large endoplasmic organelles (*arrows*). An actin-free indifferent zone is shown in **A** (*asterisk*)

Fig. 6A,B. Actin bundles in the basal zone of live rhizoids after microinjection of Bodipy phallacidin. Projection of 8 serial images at 0.8-μm intervals in the first (**A**) and second half (**B**) of the basal cell cylinder. One large and one very small actin ring is visualized in the streaming endoplasm and these are associated with large organelles (*arrows*) that momentarily stopped moving

move through the actin MF array without dragging it along. Neither the sedimenting statoliths nor the gravitropic downward bending tip of the rhizoid drastically changed the immunofluorescently labeled MF arrangement. The apical actin patch was not displaced from its central position in the tip; it remained in the stable position in the centre of the downward bending rhizoid (Fig. 4).

Actin in the basal regions of rhizoids

After labeling the basal zone with rhodamine phalloidin (Fig. 5), projections of serial images revealed two hemicylindrical peripheral arrays of thick, interconnected actin MF bundles separated by two actin-free regions or indifferent zones. In addition to the subcortical actin bundles, actin was also detected in the streaming endoplasm in the form of ring-like structures associated with the surface of larger organelles, presumably plastids. Actin rings, however, were not visualized after chemical fixation and immunolabeling (not shown).

Microinjection with low amounts of Bodipy FL phallacidin and FITC-phalloidin also resulted in labeling of actin MF bundles in the basal zone of live actively streaming cells (Fig. 6). The actin pattern was very similar to that observed after immunofluorescence and rhodamine phalloidin labeling (compare Fig. 6 and Fig. 5). Since cytoplasmic streaming was not impeded after microinjection, actin rings could only be documented on the surface of those organelles which had stopped moving for a few seconds (Fig. 6A, arrows). Labeling of actin arrays in the relatively stationary cytoplasm of the subapical and apical zone of rhizoids by microinjection was not successful in that low amounts of Bodipy phallacidin or FITC-phalloidin did not produce a detectable fluorescence pattern and higher concentrations caused cessation of tip growth and breakdown of cytoplasmic streaming.

Microtubular cytoskeleton in rhizoids

Immunofluorescence. Serial optical sectioning by confocal microscopy confirmed that the apical zone is completely devoid of immunofluorescently stainable MTs. A dense array of predominantly axially oriented but occasionally reticulate MTs occupied the subapical cytoplasm (Fig. 7A,B). Microtubules were dispersed uniformly throughout this region and no difference in the density of MTs in the cortical as compared to the inner cytoplasm could be observed. The nucleus and other organelles are closely associated with numerous MTs (Fig. 7B). Multiple tubulin-rich spots dispersed over the basal face of the nucleus in a small number of rhizoids are suggestive of MT nucleating or anchoring sites (arrows in Fig. 7B). Similar structures were not found on the apical side of the nucleus. In some rhizoids, a single bundle of MTs was detected inside the nucleus close to the nucleolus (Fig. 8) without any connections to the cytoplasmic MT system. In the basal zone, short branching clusters of MTs formed two cortical hemicylinders that are separated by the two different zones, the areas between the oppositely moving streams of endoplasm, which are essentially devoid of MTs (Fig. 7C).

Microinjection of fluorescent brain tubulin. After microinjecting carboxyfluorescein-tubulin into the basal zone of rhizoids, MTs assembled from a band-like structure at the basal face of the nucleus approximately 10 min after microinjection, and extended towards the base of the cell (Fig. 9A). At 30 min after microinjection, MTs had increased in number and density and weakly fluorescing MTs were detected in the thin cytoplasmic layer between the nuclear and plasma membrane (Fig. 9B, arrows). Eventually, MTs were also observed in the subapical

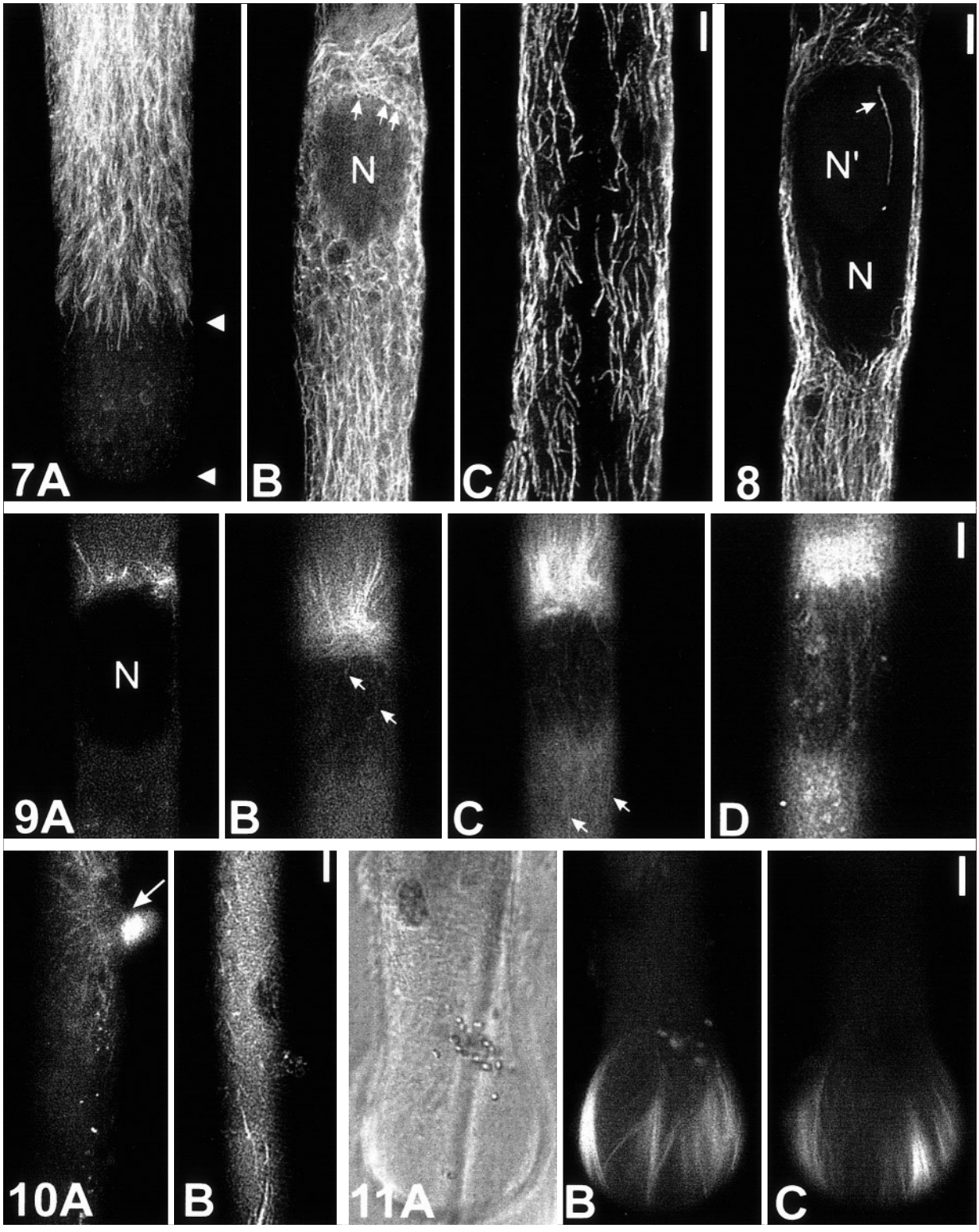

cytoplasm (Fig. 9C). After 1 h, an extensive MT pattern was visualized in the basal zone (not shown), the nuclear region and throughout the subapical cytoplasm (Fig. 9D).

In the cortical cytoplasm of the basal zone, at first, MTs radiated from the injection site (Fig. 10A) and later, short, branched MTs were observed which seem to originate from multiple, obviously independent, nucleation sites near the plasma membrane (Fig. 10B).

Termination of tip-growth and tip-swelling, which often occurred after microinjection, was accompanied by MT polymerization in the apex (Fig. 11). However, MTs did not appear in the apex of rhizoids showing unimpeded tip growth.

Figs. 7–11. Distribution of MTs in *Chara* rhizoids. Scale bars = 10 μm

Fig. 7A–C. Anti-tubulin immunofluorescence in the various regions of a *Chara* rhizoid. **A,B** Except for the MT-free apical zone (region between the arrowheads in **A**), mainly axially oriented MTs are present as a dense network encircling the nucleus (*N* in **B**) and other organelles (indicated by dark spherical regions) in the subapical zone. *Arrows* (**B**) indicate putative MT nucleating centres at the basal side of the nuclear envelope. Optical sections of 0.6 μm thickness. **C** Projection of 12 serial images at 0.8-μm intervals showing the cortical, short branching clusters of MTs in the basal hemicylinder of a rhizoid. The indifferent zone is indicated by the absence of MTs

Fig. 8. Anti-tubulin immunofluorescence reveals the presence of an MT structure (*arrow*) inside the nucleus (*N*) at the surface of the nucleolus (*N′*). Projection of six serial images at 0.42-μm intervals

Fig. 9A–D. Fluorescence images of the nuclear region (*N* = nucleus) collected 20 min (**A**), 40 min (**B**), 50 min (**C**) and 60 min (**D**) after injecting fluorescently labeled tubulin into the basal zone of a live rhizoid. **A** Short basipetally elongating MTs are polymerized from a broad band-like nucleation site at the basal side of the nuclear envelope. **B** The MTs elongate further and additional weakly fluorescing MTs are visualized in the thin cytoplasmic layer between nuclear and plasma membrane (*arrows*). **C** A great density of MTs growing in the basal direction and some in the apical direction (*arrow*) are labeled in the subapical cytoplasm. **D** Numerous MTs are also labeled throughout the subapical cytoplasm, but they are difficult to visualize because of the low detector settings suited to the fluorescence of the MTs concentrated near the nucleus

Fig. 10A,B. Fluorescence images of the basal zone of a rhizoid after injection of fluorescently labeled exogenous tubulin. **A** At 20 min after injection, fluorescing MTs are visualized radiating from the injection site (*arrow*) in the basal zone. **B** At 40 min after injection, fluorescent tubulin has incorporated into numerous short MTs that are spread throughout the cortical cytoplasm of the basal zone

Fig. 11A–C. Images of a rhizoid that stopped tip growth and developed tip-swelling after injection of fluorescently labeled tubulin. **A** Brightfield image corresponding to the two fluorescence images of subsequent focal planes. **B,C** Microtubules have elongated into the apical zone during cessation of tip growth

Compared to immunofluorescence, microinjection revealed relatively few MTs in rhizoids. In parallel control injections into internodal cells from the same species, fluorescent tubulin from the same aliquots routinely incorporated more quickly into the MT arrays, and MT numbers and patterns appeared the same as in immunofluorescently labeled rhizoids (not shown; see also Kropf et al. 1997).

Actin cytoskeleton in protonemata

Upward growing protonemata have the same basic arrangement of actin filaments as downward growing rhizoids (compare Fig. 12A with Fig. 4A). A dense actin MF network, shown in a median (Fig. 12A) and a peripheral focal plane (Fig. 12B), was labeled throughout the subapical cytoplasm by immunofluorescence. In a very thin (0.2 μm) optical section of the subapical zone (Fig. 13), predominantly axially oriented actin MF bundles are shown to be closely associated with organelles. Actin MFs appear thicker and less reticulate in the apical cytoplasm and focus into a well-defined actin patch in the centre of the apical dome (Fig. 12A) just as occurs in rhizoids (Fig. 4). In most protonemata, the apical zone (30–35 μm) was shorter than in rhizoids (40–45 μm). The thick undulating actin MF bundles of the basal zone also resemble those in rhizoids (Fig. 14; compare with Figs. 5, 6). Endoplasmic actin rings, however, were not detected in protonemata after chemical fixation and immunolabeling.

Microtubular cytoskeleton in protonemata

Like the actin cytoskeleton and the cytoplasmic organization, the MT cytoskeleton of dark-grown protonemata also strikingly resembles that of rhizoids (Fig. 15, compare with Fig. 7). In most protonemata, the MT-free apical zones are shorter than those in rhizoids. This could be because protonemata generally grow more slowly than rhizoids; the length of the apical and subapical zone is positively correlated to the growth rates. The basal zone has a cortical MT array consisting of short, mostly axially oriented MTs, that are frequently arranged in small branching clusters. The cylindrical array is interrupted by the two indifferent zones, just as in rhizoids (compare Fig. 15C with Fig. 7C).

Discussion

Confocal laser scanning microscopy was used for detailed investigations on the complex three-dimensional organization of the actin and microtubule cytoskeleton in rhizoids and protonemata of characean green algae. The cytoskeleton of negatively gravitropic protonemata was also demonstrated for the first time in order to compare its organization with positively gravitropic rhizoids. Previous studies using conventional fluorescence microscopy failed to resolve the fine details of filamentous cytoskeletal elements, which are densely packed and cause strong out-of-focus blur especially in the stationary cytoplasm of the apical and subapical zones. The capacity of confocal laser scanning microscopy for optical sectioning was indispensable for studying the spatial arrangement of the cytoskeleton in both rhizoids and protonemata.

Although MBS has been described as a cross-linker (Sonobe and Shibaoka 1989) that improves the preservation and visualization of actin in many cell types, MBS was of limited use in protonemata and rhizoids because the usually applied concentrations negatively affected the stability of the MT cytoskeleton (Collings et al. 1995) and caused breakdown of the cytoplasmic zonation (Braun and Sievers 1994). Therefore, the incubation time and the MBS concentration had to be drastically reduced which resulted in only slightly improved actin labeling. The best results for visualization of actin were obtained by using a fixative solution containing high-grade glutaraldehyde which was freshly thawed from −20 °C (according to Wasteneys et al. 1996). Extensive arrays of actin MFs were visualized by immunofluorescence in all cytoplasmic zones of rhizoids

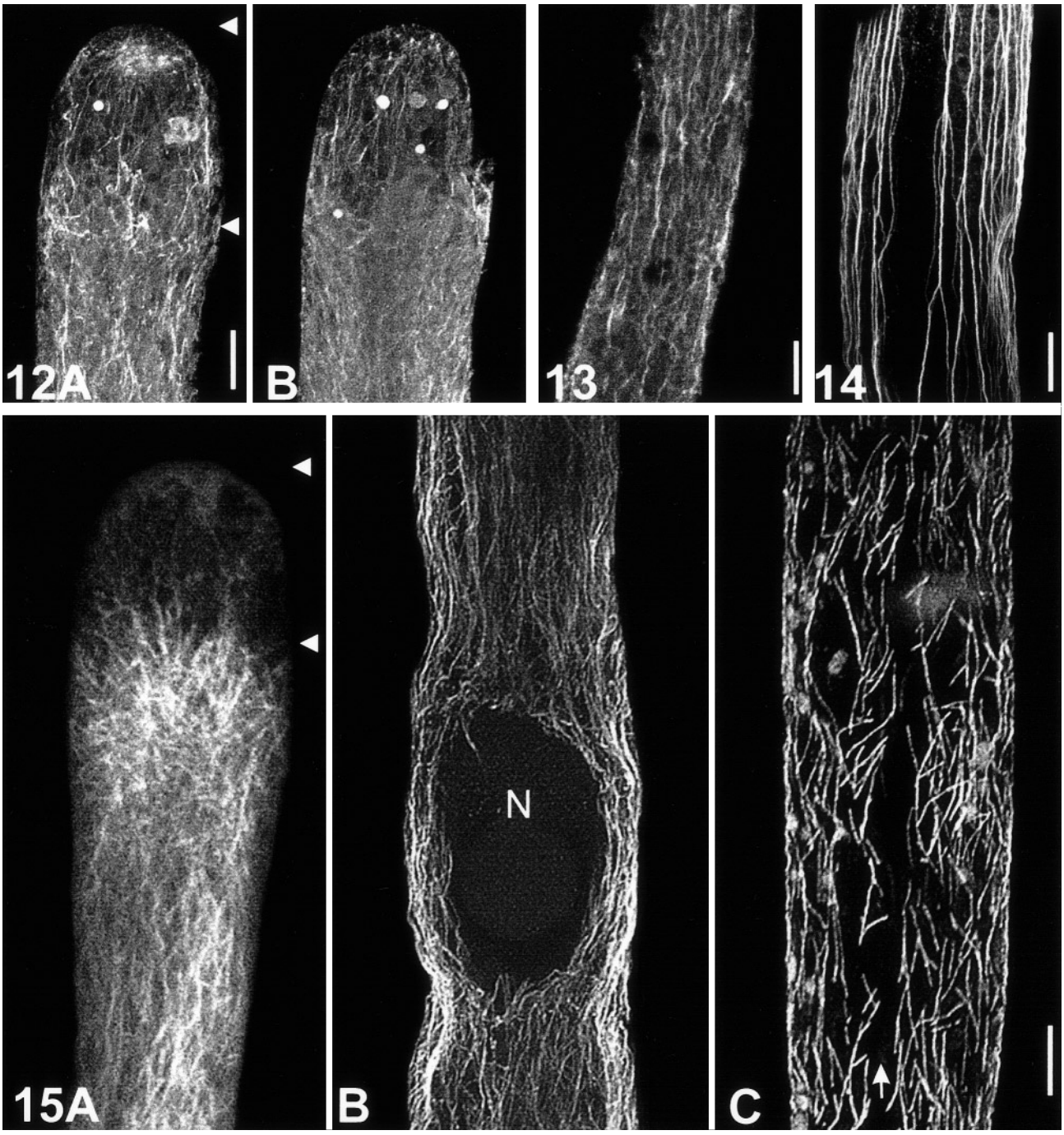

and protonemata which were well preserved by this method.

The distribution of the actin and MT cytoskeleton reflects the polar organization and cytoplasmic zonation of positively gravitropic (downward bending) rhizoids and negatively gravitropic (upward bending), dark-grown protonemata. Except for a shorter apical zone in protonemata, both cell types correspond perfectly in their polar cytoplasmic and cytoskeletal organization. The two subcortical arrays of interconnected actin MF bundles responsible for the rotational cytoplasmic streaming in rhizoids has already been well documented by rhodamine phalloidin labeling (Tewinkel et al. 1989; Sievers et al. 1991a). Microinjection of fluorescent phallotoxins and immunofluorescence showed essentially the same basal actin organization in protonemata. In addition, ring-like actin structures associated with large organelles, plastids and/or mitochondria, in the streaming endoplasm were detected for the first time by rhodamine phalloidin labeling and microinjection of live rhizoids. Actin rings were not observed after chemical fixation and immunofluorescence. In internodal cells of *Nitella* but not in *Chara*, nucleus-associated actin rings have been observed in the vigorously streaming endoplasm (Wasteneys and Williamson 1991). The possibility has been discussed that the actin

Figs. 12–15. Actin and MT organization in *Nitella* protonemata. Scale bars = 10 μm

Fig. 12A,B. Anti-actin immunofluorescence of the apical and subapical zone of a protonema in a median (**A**) and peripheral focal plane (**B**). Mainly axially oriented actin MF bundles form a dense network in the subapical cytoplasm. The apical zone (region between the *arrowheads*) contains less-numerous and less-reticulate MF bundles converging into a brightly fluorescing, apical actin patch (**A**)

Fig. 13. Anti-actin immunofluorescence showing numerous actin MF bundles associated with cytoplasmic organelles (dark spheres) in a 0.2-μm thin optical section of the subapical zone

Fig. 14. Immunofluorescence image of thick actin MF bundles in the basal zone of a protonema. Two arrays of thick interconnected MF bundles are separated by the actin-free indifferent zone. Projection of ten serial images at 0.8-μm intervals

Fig. 15A–C. Anti-tubulin immunofluorescence in the various regions of a protonema. The apical zone (region between two *arrowheads*) is devoid of MTs **(A)** An extensive dense network of mainly axially oriented MTs is visualized in the 0.42-μm thin mid-plane focus images in the subapical zone (**A,B**) surrounding the nucleus (*N*). A cortical cylinder of short branching MT clusters is labeled in the basal zone (**C**). The small indifferent zone is characterized by the absence of MTs (*arrow*). Projection of ten serial images at 0.6-μm intervals

rings are responsible for nuclear rotation, a conspicuous phenomenon characteristic of *Nitella* but not *Chara* nuclei (Wasteneys and Williamson 1991 and references therein), but a role for the endomitotic replication of the nuclei appeared unlikely because the actin rings are long-lasting structures that do not delineate the constricting regions of the dividing nuclei (Wasteneys and Williamson 1991). In contrast to internodal cells, rhizoids and protonemata have only one large nucleus in a stable position at the posterior end of the subapical zone and their plastids in the basal zone do not form a layer in the cortical cytoplasm but are included in the streaming endoplasm. Therefore, although it is likely that the actin rings observed in rhizoids are associated with plastids, their function is still unknown.

Numerous, predominantly axially oriented MTs form a dense array in the subapical cytoplasm and a cortical cylinder of short, branching MT clusters in the basal zone of antibody-labeled rhizoids and protonemata (see also Braun and Sievers 1994). Interestingly, individual MT bundles were also found inside the nucleus without any contacts to the cytoplasmic MT array. The finding may relate to reports of closely packed arrays of microtubular structures inside the nuclei of *Chara* visualized by electron microscopy (Pickett-Heaps 1975) whose signification is still completely unknown.

Using two different tubulin-specific antibodies, neither conventional nor confocal microscopy detected MTs in the apical zone of rhizoids. The absence of MTs was interpreted as an adaptation to gravitropic tip growth allowing fast lateral sedimentation of statoliths which exclusively occurs in the MT-devoid apical zone (Braun and Sievers 1994). Loading rhizoids with fluorescently labeled exogenous tubulin by microinjection and subsequent confocal imaging revealed the assembly of MTs in the different zones of rhizoids. Microtubules polymerized from multiple nucleation sites at the plasma membrane in the basal zone. In the subapical zone, however, polymerization of MTs started from a well-defined nucleation centre at the basal side of the nuclear envelope. From there, at first, MTs extended towards the basal zone and, later, fanned out throughout the subapical cytoplasm showing a dynamically changing pattern of MTs. The results are supported by the visualization of a broad band of multiple sites of MT anchorage or nucleation at the basal side of the nuclear envelope of antibody labeled rhizoids. No comparable arrays were detected at the apical side of the nucleus. Very similar MT structures have been reported on the nuclear membrane of *Haemanthus* endosperm cells (Lambert et al. 1990) and MT assembly sites have been identified on the nuclei of *Nitella* internodal cells (Wasteneys et al. 1989; Wasteneys and Williamson 1989). Our results suggest the existence of two independent populations of MTs, a subapical system originating from a nucleation site located at the basal nuclear envelope and a second basal system assembling from multiple sites dispersed along the plasma membrane. In *Nitella* internodal cells, polymerization of exogeneous tubulin from multiple sites in the cortical cytoplasm was demonstrated by Wasteneys and Williamson (1989). The subapical MT system of rhizoids and protonemata is subjected to dynamic changes throughout cell division whereas the basal system remains relatively stable (data not shown). The occurrence of MTs in the apical zone after microinjection is correlated to tip swelling and the loss of gravitropic tip growth and is also described during cessation of tip growth in light-stimulated protonemata (data not shown). Exclusion of MTs from the apex therefore might be an important feature for the maintenance of tip growth.

In contrast to tubulin microinjection in characean internodal cells (Wasteneys et al. 1993; Kropf et al. 1997) exogenous tubulin incorporated relatively slowly into the microtubule arrays of rhizoids. Even after considerable incubation times, the microtubules containing fluorescent tubulin subunits probably only reflected a subset of the total number of microtubules in these cells, as judged by comparison with immunofluorescence images. This suggests that in comparison to the microtubules in diffusely expanding internodal cells, microtubules in tip-growing rhizoids and protonemata turn over relatively slowly or are slow to incorporate free tubulin.

The observation that inhibitor-induced breakdown of the MT cytoskeleton resulted in a major rearrangement of the actin cytoskeleton, but not vice versa (Braun and Sievers 1994), indicates that the relatively static MT cytoskeleton has a function not only in maintaining a constant distance of the nucleus from the cell tip but also in stabilizing the cytoplasmic polarity and the position of the subapical organelles. Microtubules might also influence the arrangement of the network of actin MFs at least in the subapical zone (Braun and Sievers 1994). Furthermore, the absence of MTs in the apical zone could explain the presence of thicker MF bundles which merge into a conspicuous actin patch close to the cell vertex, where the tip-growth-organizing complex, the Spitzenkörper, is located. The existence of the dense

patch-like array of actin in the tip of rhizoids has already been indicated by conventional fluorescence microscopy in rhodamine-phalloidin-labeled rhizoids (Sievers et al. 1991a), but only through optical sectioning and the improved labeling techniques of this study have we been able to detail the organization of the actin cytoskeleton in the apical dome, which probably reflects the most complex pattern described to date in a tip-growing cell. The actin patch coincides spatially with the aggregation of ER membranes that represents the structural centre of the Spitzenkörper (Bartnik and Sievers 1988; Braun 1996b), a finding that has not yet been observed in other tip-growing plant cell systems. The disappearance of the ER aggregation and sedimentation of statoliths onto the apical cell wall after inhibition of the actin MF system in rhizoids (Hejnowicz and Sievers 1981; Bartnik and Sievers 1988) is good evidence that actin is essential for maintaining and organizing the complex mechanism of gravitropic tip growth.

A longitudinal or oblique orientation of actin MFs and MTs is common in the cylindrical region of most tip-growing cells, but the distribution of actin MFs and MTs differs remarkably in their apices. Although dense actin networks have been reported at the tips of numerous tip-growing cells (for review, see Steer 1990) including moss protonemata (Doonan et al. 1988; Walker and Sack 1995), fern rhizoids (Kadota and Wada 1989), *Fucus* rhizoids (Kropf et al. 1989), and fungal hyphae (Heath 1987; Jackson and Heath 1990), there is increasing evidence for an actin-free zone at the apex of tip-growing cells (Robertson 1992; Jackson and Heath 1993; Meske and Hartmann 1995; Meske et al. 1996). A prominent role for actin in tip growth in pollen tubes has been questioned, because actin MFs are present throughout the length of the pollen tube except in the short apical region which is essentially devoid of them (Miller et al. 1996).

In the present study, the complex structural organization of actin MFs in the apices of rhizoids and protonemata of characean algae was demonstrated in both cell types. The orientation of actin MFs radiating from the actin patch is in accordance with the observation of shuttle-like movements of vesicles containing cell wall material between the central ER aggregation and the apical plasma membrane (Bartnik et al. 1990). Thus, it seems likely that actin not only stabilizes and organizes the Spitzenkörper, but is also important for the spatial control of actomyosin-mediated vesicle transport and exocytosis, thereby regulating cell shape and diameter.

In this respect, it may be worthwhile to consider the 'vesicle-supply-centre concept' of tip growth (Bartnicki-Garcia 1990) which suggests that the actin cytoskeleton may either anchor the vesicle-supply-centre, or Spitzenkörper, to the apical pole (pulling mechanism) or it may provide a scaffolding for the continuous advance of the vesicle-supply-centre (pushing mechanism). Since the actin cytoskeleton forms a complex, well-defined structure in the apical dome and because of the apparent lack of direct structural linkages to the apical plasma membrane, the mechanism of pushing the Spitzenkörper of rhizoids and protonemata forward seems more attractive. Tight linkage of the actin cytoskeleton to the apical plasma membrane is unlikely because the actin cytoskeleton, including the apical actin patch, was easily detached from the apical plasma membrane after plasmolysis. Considering the rates of tip growth, it is most likely that the actin cytoskeleton is only tenuously linked to the apical plasma membrane via associated proteins and integral membrane proteins like annexins (Clark et al. 1995) and integrins (Kaminskyi and Heath 1995) which are postulated to mediate exocytotic processes and to stabilize the fast-growing plasma membrane.

In gravistimulated rhizoids, reorientation of actin MFs was not observed and the actin patch remained in a stable position during gravitropic bending. The position of statoliths is important for gravity perception in rhizoids (Hejnowicz and Sievers 1981; Sievers et al. 1991b; Braun and Sievers 1993). The lateral sedimentation of statoliths, however, is not restricted in the MT-free apical zone, and they fall passively through the axially oriented MFs bundles without changing their own symmetric distribution. Since the change in growth direction (gravitropic curvature) results from differential growth on the opposite subapical flanks and because this is induced by sedimentation of statoliths in a marginal region of the apical dome, it is unlikely that the Spitzenkörper itself can be directly involved in the gravitropic component of tip growth. It is also unlikely that the actin cytoskeleton is directly involved in the primary steps of gravitropism, even though tip growth per se relies on the structure and function of MTs and actin MFs. For instance, the position of statoliths in rhizoids is controlled by the actomyosin system (Braun 1996a) but the mechanism by which differential growth of the subapical flanks is established after sedimentation of statoliths is still unknown. Whether simple blockage of vesicle exocytosis by statolith sedimentation occurs (Sievers et al. 1979; Sievers and Schnepf 1981) or whether electrical or mechanical effects on membrane channel-proteins are involved, still needs to be clarified.

There is even less information on the mechanism of negative gravitropism in protonemata. Work on the effect of gravistimulation on the distribution of actin MFs is in progress; however, it is already known that actin plays a more direct role in negatively gravitropic tip growth of protonemata because the active transport of sedimenting statoliths into the apical dome is actin dependent (Hodick 1994; Sievers et al. 1996). Actin might also mediate the displacement of the centre of maximal growth to the upper flank following the apical intrusion and sedimentation of statoliths. In contrast, the actin cytoskeleton in rhizoids actively prevents statoliths from invading the apical dome and stabilizes the apical, central position of the Spitzenkörper during gravitropic curvature (Braun 1996a). In accordance with this, it was demonstrated that rhizoids can be forced to grow in a protonema-like manner when the cytoskeletal forces that keep the statoliths out of the apical dome are overcome by centrifugal forces (Braun 1996a). If the actin MFs in protonemata are actively involved in the displacement of the Spitzenkörper and the centre of

maximal growth to the future growth direction, it should be expected that a reorientation of MFs will precede gravitropic changes in cell shape. In fact, during the phototropic response of moss protonemata, a reorientation of the apical collar-like organized MFs was observed indicating the future growth direction (Meske and Hartmann 1995; Meske et al. 1996). A spatial reorientation of the calcium gradient towards the direction of irradiation in the apex preceded the reorientation of the apical actin MFs (Meske et al. 1996; Sinclair and Trewavas 1997). The situation might be similar in characean protonemata except that apical intrusion and sedimention of statoliths might induce a rearrangement of the tip-high calcium gradient, which is essential for tip-growing cells (Herth et al. 1990; Hepler 1997; Sinclair and Trewavas 1997) by interacting with sensitive Ca^{2+} channels in the apical plasma membrane. Knowledge about Ca^{2+}-dependent, cytoskeleton-associated proteins in tip-growing cells is limited. Myosin-like proteins have been detected attached to the surface of statoliths and as a diffuse immunofluorescence array in the apical dome of rhizoids (Braun 1996b). Annexins, which have been found in pollen tube tips (Clark et al. 1995), are candidates for proteins that mediate the Ca^{2+}-dependent process of tip-focused vesicle fusion. Integral plasma membrane integrin-like molecules, which in animal cells are linked with the cytoskeleton, were detected in a tip-to-base gradient in tip-growing fungal hyphae (Kaminskyi and Heath 1995) and seem to be present in *Chara* rhizoids (Katembe et al. 1997). In conclusion, opposite gravitropism in rhizoids and protonemata is based on a structurally very similar cytoskeletal organization of actin MFs and MTs in both cell types. The opposite direction of gravitropic tip growth might, therefore, depend on the activities of associated proteins that regulate the action and properties of the actin cytoskeleton and the processes involved in the spatial control of tip growth in a calcium-dependent manner.

The authors are grateful to Prof. A. Sievers, Prof. D. Menzel, Dr. B. Buchen and Dr. R.E. Williamson for many helpful comments and critical reading of the manuscript and Prof. B.E.S. Gunning for providing help and skillful support with the confocal microscope. This work was financially supported by a research grant from the Deutsche Forschungsgemeinschaft to M.B. (DFG Br 1637/1-1), a Queen Elizabeth II Fellowship to G.O.W. and the project AGRAVIS by Deutsche Agentur für Raumfahrtangelegenheiten, DARA, Bonn, and Ministerium für Wissenschaft und Forschung, Düsseldorf.

References

Bartnicki-Garcia S (1990) Role of vesicles in apical growth and a new model of hyphal morphogenesis. In: Heath IB (ed) Tip growth in plant and fungal cells. Academic Press, San Diego, pp 211–232

Bartnik E, Sievers A (1988) In-vivo observation of a spherical aggregate of endoplasmic reticulum and of Golgi vesicles in the tip of fast-growing *Chara* rhizoids. Planta 176: 1–9

Bartnik E, Hejnowicz Z, Sievers A (1990) Shuttle-like movements of Golgi vesicles in the tip of growing *Chara* rhizoids. Protoplasma 159: 1–8

Braun M (1996a) Anomalous gravitropic response of *Chara* rhizoids during enhanced accelerations. Planta 199: 443–455

Braun M (1996b) Immunolocalization of myosin in rhizoids of *Chara globularis* Thuill. Protoplasma 191: 1–8

Braun M (1997) Gravitropism in tip-growing cells. Planta 203: S11–S19

Braun M, Sievers A (1993) Centrifugation causes adaptation of microfilaments; studies on the transport of statoliths in gravity sensing *Chara* rhizoids. Protoplasma 174: 50–61

Braun M, Sievers A (1994) Role of the microtubule cytoskeleton in gravisensing *Chara* rhizoids. Eur J Cell Biol 63: 289–298

Buchen B, Braun M, Hejnowicz Z, Sievers A (1993) Statoliths pull on microfilaments. Experiments under microgravity. Protoplasma 172: 38–42

Clark GB, Turnwald S, Tirlapur UK, Haas CJ, von der Mark K, Roux SJ, Scheuerlein R (1995) Polar distribution of annexin-like proteins during phytochrome-mediated initiation and growth of rhizoids in the ferns *Dryopteris* and *Anemia*. Planta 197: 376–384

Collings DA, Wasteneys GO, Williamson RE (1995) Cytochalasin rearranges cortical actin of the alga *Nitella* into short stable rods. Plant and Cell Physiol 36: 765–772

Doonan JH, Cove DJ, Lloyd CW (1988) Microtubules and microfilaments in tip growth: evidence that microtubules impose polarity on protonemal growth in *Physcomitrella patens*. J Cell Sci 89: 533–540

Heath IB (1987) Preservation of a labile cortical arrays of actin filaments in growing hyphal tips of the fungus *Saprolegnia ferax*. Eur J Cell Biol 44: 10–16

Hejnowicz Z, Sievers A (1981) Regulation of the position of statoliths in *Chara* rhizoids. Protoplasma 108: 117–137

Hepler PK (1997) Tip growth in pollen tubes: calcium leads the way. Trends Plant Sci 3: 79–80

Hepler PK, Cleary AL, Gunning BES, Wadsworth P, Wasteneys GO, Zhang DH (1993) Cytoskeletal dynamics in living plant cells. Cell Biol Int 17: 127–142

Herth W, Reiss H-D, Hartmann E (1990) Role of calcium ions in tip growth of pollen tubes and moss protonema cells. In: Heath IB (ed) Tip growth in plant and fungal cells. Academic Press, San Diego, pp 91–118

Hodick D (1993) The protonema of *Chara fragilis* Desv.: regenerative formation, photomorphogenesis, and gravitropism. Bot Acta 106: 388–393

Hodick D (1994) Negative gravitropism in *Chara* protonemata and rhizoids: a model integrating the opposite gravitropic responses of protonemata and rhizoids. Planta 195: 43–49

Jackson SL, Heath IB (1990) Effects of exogenous calcium ions on tip growth, intracellular Ca^{2+} concentrations and actin arrays in hyphae of the fungus *Saprolegnia ferax*. Exp Mycol 13: 1–12

Jackson SL, Heath IB (1993) The dynamic behavior of cytoplasmic F-actin in growing hyphae. Protoplasma 173: 23–34

Kadota A, Wada M (1989) Circular arrangement of cortical F-actin around the subapical region of a tip-growing fern protonemal cell. Plant Cell Physiol 30: 1183–1186

Kaminskyi SGW, Heath IB (1995) Integrin and spectrin homologues, and cytoplasm-wall adhesion in tip growth. J Cell Sci 108: 849–856

Katembe WJ, Swatzell LJ, Makaroff CA, Kiss JZ (1997) Immunolocalization of integrin-like proteins in *Arabidopsis* and *Chara*. Physiol Plant 99: 7–14

Kropf DL, Berge SK, QuatranoS RS (1989) Actin localization during *Fucus* embryogenesis. Plant Cell 1: 191–200

Kropf DL, Williamson RE, Wasteneys GO (1997) Microtubule orientation and dynamics in elongating characean internodal cells following cytosolic acidification, induction of pH bands, or premature growth arrest. Protoplasma 197: 188–198

Lambert AM, Vantard M, Schmidt AC, Stoeckel H (1990) Mitosis in plants. In: Lloyd CW (ed) The cytoskeletal basis for plant growth and form. Academic Press, London, pp 199–208

Lessard JL (1988) Two monoclonal antibodies to actin: one muscle selective and one generally reactive. Cell Motil Cytoskel 10: 349–362

Meske V, Hartmann E (1995) Reorganization of microfilaments in protonemal tip cells of the moss *Ceratodon purpureus* during the phototropic response. Protoplasma 188: 59–69

Meske V, Ruppert V, Hartmann E (1996) Structural basis of the red light induced repolarization of tip-growth in caulonema cells of *Ceratodon purpureus*. Protoplasma 192: 189–198

Miller DD, Lancelle SA, Hepler PK (1996) Actin microfilaments do not form a dense meshwork in *Lilium longiflorum* pollen tube tips. Protoplasma 195: 123–132

Pickett-Heaps JD (1975) Green algae. Structure, reproduction and evolution in selected genera. Sinauer Associates. Sunderland, Massachusetts

Robertson RW (1992) The actin cytoskeleton in hyphal cells of *Sclerotium rolfsii*. Mycologia 84: 41–51

Sievers A, Schnepf E (1981) Morphogenesis and polarity of tubular cells with tip growth. In: Kiermayer O (ed) Cytomorphogenesis in plants (Cell biology monographs, vol 8). Springer, Wien New York, pp 265–299

Sievers A, Heinemann B, Rodriguez-Garcia MI (1979) Nachweis des subapikalen differentiellen Flankenwachstums im *Chara*-Rhizoid während der Graviresponse. Z Pflanzenphysiol 91: 435–442

Sievers A, Kramer-Fischer M, Braun M, Buchen B (1991a) The polar organization of the growing *Chara* rhizoid and the transport of statoliths are actin-dependent. Bot Acta 104: 103–109

Sievers A, Buchen B, Volkmann D, Hejnowicz Z (1991b) Role of the cytoskeleton in gravity perception. In: Lloyd CW (ed) The cytoskeletal basis for plant growth and form. Academic Press, London, pp 169–182

Sievers A, Buchen B, Hodick D (1996) Gravity sensing in tip-growing cells. Trends Plant Sci 1: 273–279

Sinclair W, Trewavas AJ (1997) Calcium in gravitropism. A re-examination. Planta 203: S85–S90

Sonobe S, Shibaoka H (1989) Cortical fine actin filaments in higher plant cells visualized by rhodamine-phalloidin after pretreatment with *m*-maleimidobenzoyl-N-hydroxysuccinimide ester. Protoplasma 148: 80–86

Steer MW (1990) Role of actin in tip growth. In: Heath IB (ed) Tip growth in plant and fungal cells. Academic Press, San Diego, pp 110–145

Tewinkel M, Kruse S, Quader H, Volkmann D, Sievers A (1989) Visualization of actin filament pattern in plant cells without prefixation. A comparison of differently modified phallotoxins. Protoplasma 149: 178–182

Vigers GPA, Coue M, McIntosh JR (1988) Fluorescent microtubules break up under illumination. J Cell Biol 107: 1011–1024

Walker LM, Sack FD (1995) Microfilament distribution in protonemata of the moss *Ceratodon*. Protoplasma 189: 229–237

Wasteneys GO, Williamson RE (1989) Reassembly of microtubules in *Nitella tasmanica*: assembly of cortical microtubules in branching clusters and its relevance to steady state microtubule assembly. J Cell Sci 93: 705–714

Wasteneys GO, Jablonsky PP, Williamson RE (1989) Assembly of purified brain tubulin at cortical and endoplasmic sites in perfused internodal cells of the alga *Nitella tasmanica*. Cell Biol Int Rep 13: 513–528

Wasteneys GO, Williamson RE (1991) Endoplasmic microtubules and nucleus-associated actin rings in *Nitella* internodal cells. Protoplasma 162: 86–98

Wasteneys GO, Gunning BES, Hepler PK (1993) Microinjection of fluorescent brain tubulin reveals dynamic properties of cortical microtubules in living plant cells. Cell Motil Cytoskel 24: 205–213

Wasteneys GO, Collings DA, Gunning BES, Hepler PK, Menzel D (1996) Actin in living and fixed characean internodal cells: identification of a cortical array of fine actin strands and chloroplast actin rings. Protoplasma 190: 25–38

Zhang D, Wadsworth P, Hepler PK (1990) Microtubule dynamics in living, dividing plant cells: Confocal imaging of microinjected fluorescent brain tubulin. Proc Natl Acad Sci USA 87: 8820–8824